Workshop

Semiconductor Advances for Future Electronics

June 7 and 8, 2018

Campus, University of Twente
Enschede, The Netherlands

Program SAFE 2018

Welcome to SAFE 2018!

Dear SAFE attendee,

SAFE is back! (and no more part of ICT.OPEN). We would like to welcome you to the SAFE 2018 workshop, held June 7 and 8, 2018 at the University of Twente, Enschede, The Netherlands.

About the workshop: SAFE is an annual workshop on Microsystems, Materials, Technology and RF-devices, which is organized within the three technical Dutch universities of Twente, Delft and Eindhoven with participation from scientist in the Benelux and Germany. The conference is organized for PhD students and is intended for them to expand their network and share their research ideas, providing a unique opportunity to form the basis for future collaborations.

Students may present already published work or new ideas, but can also feel safe to share their initial ideas without publishing them officially (of course the PhD students may choose to share their posters afterwards, on- or off-line). We encourage all PhD students to submit a poster/paper to facilitate interactions among the students.

SAFE *(Semiconductor Advances for Future Electronics)* was formerly an independent conference but later became a track of ICT.OPEN. However, as of 2018 we decided to organize the conference independently again in order to have the conference on a smaller scale and thus to better serve the interest of materials, technology and device researchers. Each year one of the technical universities will be responsible for the organization of the conference. In 2018 the SAFE workshop is held at the campus of the University of Twente. In 2019 it will be hosted by the TU Delft and in 2020 by the TU Eindhoven. Information about submission, registration and hotels is available on www.safe2018.eu.

So don't miss this great networking opportunity and we look forward to seeing you at SAFE 2018 in Twente!

SAFE 2018 organising committee

Conference chair: Gijs Krijnen - University of Twente

Programme committee chair: Paddy French - Delft University of Technology

Programme committee members:

Wolfgang Krautschneider - Technische Universität Hamburg-Harburg

Fred Roozeboom - TNO / Eindhoven University of Technology

Jurriaan Schmitz - University of Twente

Program

Thursday 7 June 2018

10.30 - 11.30	Ravelijn	Registration & Coffee
11.30 - 11.45	Ravelijn	Official opening by Paddy French
11.45 - 12.30	Ravelijn	Keynote presentation by David Fernandez Rivas
12.30 - 13.30	Drienerburght	Lunch break & Poster Session
13.45 - 14.45	Ravelijn	PhD Oral presentations
		S20: Juan J. Montero Rodríguez, *Simulation and characterization of cells by impedance spectroscopy*
		S10: H.-W. Veltkamp, *Trench-assisted surface channel technology (TASCT) as platform for high-temperature physical parameter sensing*
		S08: Gerjan Wolterink, *3D Printing soft sensing structures using FDM technologies*
14.45 - 15.45	Ravelijn	Flash presentations
15.45 - 16.00	Ravelijn	Coffee break
16.00 - 17.30	Drienerburght	Poster Session & drinks
17.30 - 18.30	Drienerburght	Something fun!
18.30 - 21.00	Drienerburght	Barbecue & drinks

Friday 8 June 2018

09.00 - 09.15	Ravelijn	Welcome & Coffee
09.15 - 10.00	Ravelijn	Invited lecture by Dr. Regina Luttge (TU/e)
10.00 - 11.00	Ravelijn	PhD Oral presentations
		S07: Viviane Silva Teixeira, *Electrical Impedance Spectroscopy Measurement of in vitro cells solutions in order to distinguish different cell types*
		S19: A.J. Onnink, *Strategies to mitigate the ammonium halide contamination of an ALD/CVD reactor*
		S06: Y. Zeng *Micro Coriolis mass flow sensor driven by integrated PZT thin film actuators*
11.00 - 11.15	Ravelijn	Poster & Flash Awards
11.15 - 11.30	Ravelijn	Coffee Break
12.30 - 12.30	Drienerburght	Posters
12.30 - 13.30	Drienerburght	Lunch

Keynote presentations

David Fernandez Rivas (University of Twente)

Bubbles aka Cavitation, and some of its applications

For many scientists ‘bubble means trouble’; for example, in a clogged microfluidic channel, or covering the electrodes’ surface in solar-to-fuel devices. I will share several cases in which different types of bubbles were tamed and yielded beneficial results.

The bubbles I work with are created either with ultrasound, laser or electrochemically. Particularly, those made with ultrasound are an important ingredient of a spin-off company I co-founded: BuBclean. Also, it seems that by using lasers to create thermocavitation, we will soon spin-out a new company based on a novel needle-free injection technology.

If I manage to answer your questions, I hope to convince you that ‘a bubble is not always trouble’.

Regina Luttge (Eindhoven University of Technology)

Brain-on-Chip: An emerging microphysiological systems technology

Brain diseases are a major burden on society. Particularly, mechanisms of cellular and molecular communication causing brain disorders are poorly understood limiting the success of therapies. I address this need by means of a nano- and microfabrication methods yielding miniaturized microphysiological systems to study brain activity in vitro.

Building forth on my ERC starting grant project MESOTAS, I will present suggestions for wiring the neuronal network properties preserved in the DNA of neuronal stem cells with artificial intelligence via integrated structural features such as electrodes and nanogrooves. Often we follow a modular approach allowing to combine different materials with designed surfaces topographies in a rapid prototyping fashion in conjunction with more costly approaches of micro- and nanoscale silicon integration for the sensors and actuators. This presentation highlights on our advances for BoC technology and reflect on the needs to take human organ and disease models on chip to the next level of their utility.

Poster Abstracts

S01: Maurits de Jong (University of Twente)

Towards Understanding the Recovery of Hot-Carrier induced Degradation by Annealing

Several long-channel nMOSFET devices of various lengths have been degraded by hot-carrier injection, resulting in a shift of the parameters (threshold voltage, maximum transconductance, subthreshold swing) of the devices. The devices have been repaired by an anneal in a nitrogen ambient, where at the original post-metal anneal temperature of T = 400 ^{o}C, the performance is fully restored. An anneal at a higher temperature induced a change to the devices, manifested in a gradual shift of the threshold voltage. Subsequent annealing at lower temperatures, did not result in the original performance, suggesting that the thermal degradation is permanent. The recovery rate is found to be independent of both the transistor gate length and the cooling rate upon annealing. These findings are used to gain further understanding of the mechanisms behind the recovery of hot-carrier damage and how to influence the recovery rate at lower temperatures.

S02: Martijn Schouten, Remco Sanders, Gijs Krijnen (University of Twente)

3D printed wearable sensors

At the moment microtechnology allows the fabrication of microscopic systems with really high complexity. However, the dimensions of the systems that can be fabricated is limited. In the future Multi-material 3D printing might be used to fabricate systems with a similar complexity, but at more macroscopic dimensions. This is useful in for example robotics, especially when focusing on medical applications since here there is a relatively large need for customization. Using a system with only two materials, we have 3D printed a capacitive force sensor, which can be used to measure forces using an oscillatory readout, as well as s-EMG electrodes, several resistive force sensors and even an electrostatically actuated oscillating cantilever. All of these sensors are made out of rubber like materials and are therefore very strong and flexible. This also makes them particularly useful in wearables. To maximize the freedom of movement that is achieved using these sensors, the electronics that read out the sensors, should be wireless and embedded in the 3D printed part. To keep the 3D printed systems flexible with the electronics in it, the electronics should be either flexible or small. A wireless system also implies that the electronics should be low power. Furthermore, to continue towards complex robotic systems, printers that can print more than two materials will need to be developed. The same holds for printers that can combine different printing techniques, since every printing technique has its own specific advantages. One important requirement for achieving this is the capability to switch printheads, since the moving part of the printer should be kept as light weight as possible. When these printers and small and efficient readout electronics become available we will get closer to fabricating soft and functional wearable devices with complex functionality.

[1] G. Wolterink, R. Sanders, F. Muijzer, B. J. van Beijnum and G. Krijnen, 3D-printing soft sEMG sensing structures, 2017 IEEE SENSORS, Glasgow, 2017, pp. 1-3.
[2] M. Schouten, R. Sanders and G. Krijnen, 3D printed flexible capacitive force sensor with a simple micro-controller based readout, 2017 IEEE SENSORS, Glasgow, 2017, pp. 1-3.
[3] B. Eijking, R. Sanders and G. Krijnen, Development of whisker inspired 3D multi-material printed flexible tactile sensors, 2017 IEEE SENSORS, Glasgow, 2017, pp. 1-3.

S03: Yu Xin, Gregory Pandraud, Linda Otten, Yongmeng Zhang & Paddy French (Delft Univ. of Technology)

Functionalized SU-8 waveguide for biomedical sensing: a plug & play diagnosis system

We present an optical system for monitoring bacteria in fluid, e.g., the existence and concentration of E.coli in patients drain fluid after colon anastomosis. Optical systems have the merit of fast response which is a defining factor in bedside diagnosis. The proposed optical system mainly includes an optical source, the sensing element, which is optical waveguide here, and a detector. The waveguide is made of SU-8 with a vertical structure. SU-8 is chosen as waveguide core material because of its suitable optical properties: transparent above 400 nm and with a refractive index of 1.57 at 1.3 μm wavelength. It is a photoresist that can be fabricated by E-beam lithography, a maskless direct writing method which can guarantee fast prototyping, sub-micron and high precision fabrication. The fabrication cost is also cut down greatly. SU-8 is very stable after polymerization, which is crucial as a chemical or biomedical sensor material. After chemical treatment, the surface of SU-8 can be functionalized with antibodies and this enables its applications in biomedical field. The waveguide was designed vertically to generate evanescent waves on both left and right surfaces for sensing. This increases the sensing area and optical energy distributed in the cladding to interact with immobilized E.coli. Both aspects will increase waveguide sensitivity. The surface of the designed waveguide can be functionalized with antibodies to immobilize specific bacteria on it. After surface functionalization and incubation with E.coli solutions of different concentrations, the waveguides absorption was measured. The results demonstrate that the waveguide is sensitive to E.coli concentration changes. In addition, tapers were designed and added to the waveguide to relieve the alignment tolerance for the aim of making a plug-and-play bedside diagnostic system.

S04: Haye Witteveen, Gijs Krijnen (University of Twente), Vitaly Svetovoy (University of Groningen)

Combustion of a hydrogen-oxygen mixture in nano-bubbles as an actuation principle

Miniaturization of systems can reduce costs, and may offer properties that larger systems do not have. Micro-actuators are required to drive these systems. Traditional actuators suffer from scaling problems on the microscale. Electromagnetic actuators become relatively weak, and existing combustion engines do not work on the microscale since reactions quench in small volumes. Recently, the reaction between hydrogen and oxygen was observed in nano- and micro-bubbles. The bubbles containing a mixture of gases were produced in microsystems using electrochemical decomposition of water with a fast switching of voltage polarity. It was observed that nano-bubbles could combust spontaneously at room temperature. Using the self-combusting properties of these nano-bubbles, a micro-actuator is fabricated which can deliver high forces by electrochemically producing gas, and can actuate fast by releasing the pressure due to self-combustion of nano-bubbles. By the use of standard microfabrication techniques, devices are made with an SU-8 membrane with a radius of 75 to 500 μm, and thickness of 5 μm. SU-8 is chosen because as a photo resist, it is easily patterned. The thickness of SU-8 can be tuned specifically, giving good control of the device dimensions. The electrodes are made of 200 nm aluminum for good conduction, and a 100 nm titanium top layer to protect the electrodes from the exploding nano-bubbles, which damage the electrodes over time.

S05: Rajeev Ranjan & Wolfgang Krautschneider (Hamburg University of Technology)

Memristive system Design

Development of memristor-based device in 2008 has encouraged scientists and engineers to perform brain-inspired cognitive tasks on the hardware level. Memristor is a resistor with memory which works fundamentally like a synapse in our brain. It can be fabricated in cross-bar array which provides a high density of the device. Since the continuous switching memristor is in its infant stage, in order to progress the research in the neuromorphic circuit an On-chip emulator has been designed. It is switched resistor based approach

where programming is done externally on FPGA. It gives freedom to program any memristive model and tests its behavior. The designed ASIC has 5 memristor emulators with one having a conductance range from 4.88 nS to 4.99 S (200 K to 204.8 M) and other 4 having conductance ranges from 195 nS to 190 S (5.2 K to 5.12 M). The emulator ASIC also has two integrate and `x000Cre` (I & F) neuron circuit on-chip to test the fundamental behavior of a neuron. This thesis introduces the memristor emulator and the realization of synapse functionalities used in neuromorphic circuits such as long term potentiation (LTP), Long Term depression (LTD) and synaptic plasticity. The Biological brain has not been fully understood, so it is realistic to implement the known functionalities of brain-like pattern recognition. An architecture based on memristor model and neuron circuit has been simulated in LTSpice to mimic the basic functionality of brain and develop pattern recognition of four different images. Each image is 4X3(12 pixels) and simulation shows successful learning.

[1] Integrated Circuit with Memristor Emulator Array and Neuron Circuits for Biologically Inspired Neuromorphic Pattern Recognition Artikel in Journal of Circuits, Systems and Computers, vol. 26, Nr. 11, 2017

[2] Integrated Circuit with Memristor Emulator Array and Neuron Circuits for Neuromorphic Pattern Recognition In Tagungsband 39th International Conference on Telecommunications and Signal Processing (TSP 2016) der IEEE, 2016, p. 265-268 Vienna, Austria, 27-29 June 2016

[3] Programmable Memristor Emulator ASIC for Biologically Inspired Memristive Learning In Tagungsband 39th International Conference on Telecommunications and Signal Processing (TSP 2016) der IEEE, 2016, p. 261-264 Vienna, Austria , 27-29 June 2016

S06: Y. Zeng, J. Groenesteijn, D. Alveringh, R.J.A. Steenwelle, K. Ma, R.J. Wiegerink, and J.C. Lötters (University of Twente)

Micro Coriolis mass flow sensor driven by integrated PZT thin film actuators

We have realized a micro Coriolis mass flow sensor that is actuated by integrated lead zirconate titanate (PZT) thin film actuators, allowing low voltage, low power actuation compared to current actuation methods. The integrated PZT thin film actuators are deposited on top of silicon-rich silicon nitride (SiRN) fluidic microchannels by pulsed laser deposition (PLD). In this paper we present the fabrication process and first characterization results, including mass flow measurements with nitrogen flow using a Polytec MSA-400 laser Doppler vibrometer and integrated capacitive readout structure to detect the Coriolis induced motion of the sensor tube. The measurement results confirm that the sensor output is proportional to mass flow up to 16 mg/min with a accuracy of 3% of the full scale.

S07: Viviane Silva Teixeira, Jan-Patrick Kalckhoff, Wolfgang Krautschneider, (Hamburg Univ. of Technology)

Electrical Impedance Spectroscopy Measurement of in vitro cells solutions in order to distinguish different cell types

The objective of this work is the measurement and modeling of -dispersion present at low frequencies in some cells solutions. In order to achieve that, the technique known as Electrical Impedance Spectroscopy (EIS) was used and an equivalent electrical circuit was extracted. Models were developed for explanation of the different states of the dispersion characteristics based on the physical behavior of biological cells. The measurement technique consists on the application of a small amplitude frequency variable electric signal to the cells solution while the impedance is measured using a potentiostat for keeping the voltage drop across the cells at a constant low level during the measurements. Additionally a four electrode terminal chamber setup (4T) was constructed [1] and used to measure the impedance spectrum of two different cell lines (HaCaT human keratinocytes and L929 mouse fribroblasts) in the frequency range 100 mHz - 1 MHz. The 4T setup was important to circumvent the double layer that builds at electrodes surface at low frequencies,

preventing the observation of the real impedance of the cells [1]. Results show that HaCaT cells have a very pronounced -dispersion while in our experiments no -dispersion was seen at L929 cells. This very different dispersion behavior may be correlated to the properties of both the cell lines. Additionally, the post processing of the experimental data allowed for the extraction of HaCaT cells specific parameters like cell membrane capacitance and resistance, cytoplasmatic resistance, relaxation frequency and relaxation time. Values for these parameters have been determined and will be given.

[1] V.S. Teixeira, J-P. Kalckhoff, W, Krautschneider, D. Schroeder. Bioimpedance Analysis of L929 and HaCaT cells in Low Frequency Range. Current Directions in Biomedical Engineering, 52nd DGBMT Annual Conference, Aachen 2018.

[2] V. S. Teixeira, J-P Kalckhoff, W. Krautschneider, D. Schroeder. Impedance Spectroscopy Measurement of Ionic Solutions in order to Distinguish between Different Ions. ICT Open, 2017.

S08: Gerjan Wolterink, Gijs Krijnen (University of Twente)

3D Printing soft sensing structures using FDM technologies

Additive manufacturing, or 3D printing, enables the creation of highly customizable structures, making it a useful tool for biomedical applications. In recent years 3D printing technologies and the number of materials have significantly grown, while costs are decreasing. One of these materials is thermoplastic poly-urethane (TPU), an elastic and flexible material suitable for fused deposition (FDM) 3D printing. To create conducive materials, the dielectric TPU materials are blended with carbon particles. With the use of multi-material printers, conductive and dielectric materials can be printed in one go. Enabling the development of customizable soft sensing structures that could be integrated into prosthetic and assistive devices. In this work, we show the development of flexible 3D printed sensors using multi-material FDM printing technologies. These sensing structures include electromyography (EMG) electrodes, force and tactile sensors.

[1] Wolterink, G., Sanders, R., Muijzer, F., van Beijnum, B. J., & Krijnen, G. (2017, October). 3D-printing soft sEMG sensing structures. In SENSORS, 2017 IEEE (pp. 1-3). IEEE. https://doi.org/10.1109/ICSENS.2017.8233935.

S09: T.V.P. Schut, R.J. Wiegerink, J.C. Lötters (University of Twente, Bronkhorst High-Tech B.V.)

Micro Coriolis Mass Flow Sensor with Differential Readout

We present a design for a Coriolis mass flow sensor (CMFS) with a differential capacitive readout. By reading out the CMFS differentially, common mode external vibrations can be cancelled out. This way the CMFS can still accurately measure flows in situations where significant external vibrations are present. Previous designs consist of a free hanging channel going along a rectangular loop [1]. The channel is fixed at its inlet and outlet. The sensor can be actuated in a so-called twist mode, resulting in vibration in a so-called swing mode due to flow-induced Coriolis forces. The new design is based on the same principle. It consists of two rectangular channel loops which are mechanically combined. Together these loops form a fully symmetrical mechanical resonator. The sensor is again actuated in the so-called twist mode while flow is applied in opposite directions through the two loops. This results in Coriolis forces in opposite directions on two sides of the combined loop. The vibration due to these Coriolis forces is measured capacitively with comb readout structures. Since the vibration will be in opposite directions on both sides of the loop, common mode external vibrations can be cancelled out. In addition to the two comb structures for readout of the Coriolis vibration, identical comb structures are present on the other two sides of the channel loop. This way actuation and detection mode vibrations can be measured independently. Having readout structures on all sides of the channel loop allows for analysis and optimization of the readout scheme. Similar to the improved readout scheme presented in [2], optimized readouts schemes may allow for improvement of the sensors sensitivity and ultimately its resolution and signal to noise ratio.

[1] Haneveld, J., et al. Modeling, design, fabrication and characterization of a micro Coriolis mass flow sensor. Journal of micromechanics and microengineering 20.12 (2010): 125001.
[2] Alveringh, Dennis, et al. Improved capacitive detection method for Coriolis mass flow sensors enabling range / sensitivity tuning. Microelectronic engineering 159 (2016): 1-5.

S10: H.-W. Veltkamp, Y. Zhao, M.J. de Boer, J. Groenesteijn, R.J. Wiegerink, J.C. Lötters (University of Twente, Bronkhorst High-Tech BV)

Trench-assisted surface channel technology (TASCT) as platform for high-temperature physical parameter sensing

High-temperature physical parameter sensing, like measuring the Wobbe Index of a fuel gas, requires a microdevice that is thermally isolated, mechanically stable, chemically inert, and it should be able to generate the desired input energy on chip. In our quest to fabricate such a chip-based Wobbe Index meter we have developed a new microfabrication platform, that allows fabrication of microchannels with rectangular-shaped cross-sections. These channels are suspended from the bulk silicon and can be heated from the sidewalls via resistive silicon heater structures and from the top via resistive platinum heaters, allowing operation at temperatures up to several hundreds of degrees Celsius. Refilled trenches are used to outline the planar geometry of the channels and sidewall heating elements. The height of the channels is determined by the thickness of the device layer of the used SOI wafer. This combination decouples the channel etch from the final shape of the channel, which are fully coupled in the conventional surface channel process [1-3]. This innovative use of refilled trenches also allows in-channel structure placement, like pillars or additional mixing structures. These pillars open up the possibility to fabricate channels with much larger width than height (even up to two orders of magnitude difference). Quickly summarized, the TASCT process consists of five main steps. The first step is the outlining of the microchannels and heater elements via trench etching and refilling, subsequently followed by microchannel and reaction chamber etching. As third, the inner walls of the microfluidic device are formed via LPCVD of silicon-rich silicon nitride. Then, the electronic connections are made and as the final step, the heated elements are etched free to create suspended and thermally isolated channels. The process is currently being performed in the MESA⁺ clean room.

[1] M. Dijkstra, M.J. de Boer, J.W. Berenschot, T.S.J. Lammerink, R.J. Wiegerink, M. Elwenspoek, A versatile surface channel concept for microfluidic applications, J. Micromech. Microeng., 17(10), pp. 19711977, 2007.
[2] J. Groenesteijn, M.J. de Boer, J.C. Lötters, R.J. Wiegerink, A versatile technology platform for microfluidic handling systems, part I: fabrication and functionalization, Microfluid. Nanofluidics, 21(7), pp. 127(112), 2017.
[3] J. Groenesteijn, M.J. de Boer, J.C. Lötters, R.J. Wiegerink, A versatile technology platform for microfluidic handling systems, part II: channel design and technology, Microfluid. Nanofluidics, 21(7), pp. 126(114), 2017.

S11: G.D. Saygin (University of Twente)

The Chemistry of Stress-Induced Leakage Current in SiO2

The reliability of gate oxide is an increasing problem since the thickness of gate oxide has been decreasing over the years while the total gate oxide per chip tends to increase. One of the major problems is stress-induced leakage current (SILC) after stressing the oxide over an extended period. SILC causes retention problems in FLASH memories. Further, in CMOS logic, this degradation causes complete loss of the insulating properties of the gate oxide which is known as hard breakdown. Besides SILC and hard breakdown , other types of degradation are soft breakdown [2] and progressive breakdown [3]. All these different kinds of degradation depends on the density of electron traps in the bulk of the oxide. SILC could be detected with stress measurements in which gradual increase in gate current is seen. Behind the SILC , the exact mechanism is still not known however the possible mechanisms are charge assisted tunneling, thermally assisted tunneling over reduced barrier height and most accepted mechanism trap assisted tunneling [1].

The aim is here to study the SILC and breakdown mechanisms in order to understand the degradation of the oxide in terms of atomic scale chemical changes. And to see if a repair of the oxide defects can be engineered.

[1] Gate Oxide Reliability of Poly-Si and Poly-SiGe CMOS Devices , Houtsma, V. E. ,14 Jan 2000 Enschede, The Netherlands: Universiteit Twente

[2] Okada K, Kawasaki S, Hirofuji Y. SSDM, 1994. p. 565567

[3] Monsieur, F., Vincent, E., Pananakakis, G., Ghibaudo, G. Wear-out, breakdown occurrence and failure detection in 18-25Å ultrathin oxides (2001) Microelectronics Reliability, 41 (7), pp. 1035-1039.

S12: Yiyuan. Zhao, H.-W. Veltkamp, M.J. de Boer, Y. Zeng, J. Groenesteijn, R.J. Wiegerink and J.C. Lötters (University of Twente, Bronkhorst High-Tech BV)

Design Principles And Fabrication Method For A Miniaturized Fuel Gas Combustion Reactor

An integrated Wobbe Index (WI) meter is desired in industries such as the central heating systems and fuel gas supplies in many countries. Miniaturized on-chip fuel gas combustion and local temperature sensing facilitate the measurement of the WI and determine the exchangeability of different fuel gases. In this abstract we report the physics and fabrication considerations for designing a miniaturized on-chip combustion reactor. State of the art studies on microscale combustion have reported that microflames suffer from flame extinction in microchannels. Therefore, in order to optimize the microflames stability, we design microchannels with large internal volumes. Silicon heaters heat up the combustor wall to provide excess enthalpy. These heaters are embedded in the thin silicon dioxide and polysilicon refilled trenches as side walls. Additional platinum heaters and temperature sensors are deposited on top of the structures for accurate heat management. The combustor is fully released from the substrate for good thermal isolation. Flexure structures are designed to both suspend the floating channels for mechanical strength, and deform flexible to relax the induced thermal stress during combustion. We developed a fabrication method called Trench-Assisted Surface Channel Technology (TASCT) to make large internal volume micro-combustor. The fabricated channels and chambers all have a rectangular cross-section. High aspect ratio trenches of 3 μm wide and 50 μm deep are the key feature to fabricate these large channels. These deep trenches can be refilled with polysilicon to function as pillars to support large membranes. These refilled trenches are also the channel sidewalls and define the desired channel shape and width. Furthermore, all the key fabrication steps have been tested and further optimized. The results for trench etch and refill, slits and channel formation, as well as isotropic cavity etching have been achieved. Future work is to fabricate a working WI meter integrated with all the fluidic connections and heat management electronics to perform combustion on the chip.

[1] Zhao, Y., Veltkamp, H. W., de Boer, M. J., Zeng, Y., Groenesteijn, J., Wiegerink, R. J., & Lötters, J. C. (2017, October). Design principles and fabrication method for a miniaturized fuel gas combustion reactor. In Conference Proceedings: The 3rd Conference on MicroFluidic Handling Systems.

[2] Veltkamp, H. W., Zhao, Y., de Boer, M. J., Groenesteijn, J., Wiegerink, R. J., & Lötters, J. C. (2017, October). Fabrication of large-volume rectangular channels using trench-sidewall technology and a SOI substrate. In Conference Proceedings.

S13: Juan J. Montero Rodríguez, W. Krautschneider (Instituto Tecnológico de Costa Rica, Hamburg University of Technology

Simulation of cell cultures by effective medium approximations using the finite-element method

The dielectric properties of biological cell cultures are measured by impedance spectroscopy. These physical quantities may be also simulated by using effective medium approximations. This theory considers the sample as a mixture of spheres of given permittivity, suspended in a medium with a different permittivity. A COMSOL©model has been created to calculate the permittivity and conductivity of cell suspensions. The model considers spherical cells, randomly positioned in a rectangular PMMA chamber with parallel-plate gold electrodes at the sides. To model each individual cell, a single-shell model has been used to describe the cellular membrane. This gives a dielectric relaxation frequency in the MHz range, often referred as the beta dispersion, modeled by the Maxwell-Garnett equation. In addition, the water molecules bound by electrostatic forces to each other cannot follow high-frequency electric fields, giving origin to the gamma dispersion. This effect is also included in the model by using the Debye relaxation equation. The model is simulated using different cell concentrations, sizes, volume fractions and cell positions, using physical constants typical for lymphocytes. More complex simulation models are proposed by using the double-shell model and inserting the nucleus and small organelles into the cells. The simulation of cells gives insights into possible interaction mechanisms of cell cultures with electromagnetic fields, and the effect of each part of the cell on the total impedance.

S14: P.A. 't Hart, J.P.G. van Dijk, M. Babaie, E. Charbon, A. Vladimirescu and F. Sebastiano (TU Delft, EPFL, Intel, ISEP, UC Berkeley)

Characterization and Model Validation of Mismatch in Nanometer CMOS at Cryogenic Temperatures

The design of interface electronics for scalable quantum computers is hampered by the absence of cryogenic device models. Especially data on device mismatch at very low temperatures is lacking. This work presents the mismatch characterization of MOSFETs in a nanometer bulk CMOS process in the temperature range from 300 K down to 4.2 K. It is shown that drain-current mismatch increases with decreasing temperature and that the Pelgrom and Croon models are able to accurately predict mismatch, even at cryogenic temperatures.

S15: Mourad Jaffar-Bandjee, Gijs Krijnen, Jérôme Casas (University of Twente, Université de Tours)

The multiscale fluid mechanics of olfaction in insects: Particle Image Velocimetry (PIV) around 3D-printed models of antennae

Volatiles perception by insects is a multiscale phenomenon. We present here our first results on the dynamics of flow around a multiscale antenna of a moth, Samia Cynthia (Saturniidae). Because of the multiscale aspects of these antennas, which span four orders of magnitude (from the 3 μm diameter of the sensillae to the 1 cm length of the whole antenna), no single additive technology able to print a whole antenna. Thus, we built two 3D physical models of different architectures, focusing either on the scale made of the main branch and the secondary branches (called ramis), and on the scale made of the ramis and the hair-like sensillae. For the same reasons as above, the overall antenna and the sensillae on it are living in very different Reynolds numbers (from 0.001 to almost 1000) for a single air flow so we decided to use Particle Image Velocimetry, both in water and oil, at different speeds to understand the structure of the flow around the antenna. From these flow profiles, we calculated the proportion of volatiles reaching the antenna and derived the efficiency of the antenna in terms of molecule capture.

S16: Gaurav Gupta and Raymond J. E. Hueting (University of Twente)

Electrostatic Doping in Dimensionally-Scaled Semiconductor Devices.

To overcome the limitations of chemical doping in nanometer-scale semiconductor devices, electrostatic doping (ED) is emerging as a broadly investigated alternative to provide regions with a high electron or hole

density in a semiconductor device. In this work, we will review various reported ED approaches and related device architectures in different material systems. We will highlight the role of metal and semiconductor workfunctions, energy bandgap, and applied electric field and the interplay between them for the induced ED. In addition, we will discuss the performance benefits of ED devices and the major roadblocks of these approaches for potential future CMOS technology.

[1] G. Gupta, B. Rajasekharan, and R. J. E. Hueting, Electrostatic doping in semiconductor devices, IEEE Trans. Electron Devices, vol. 64, no. 8, pp. 30443055, Aug. 2017.

S17: Sourish Banerjee, Antonius A. I. Aarnink, Gerard Kip, Dirk J. Gravesteijn, Jurriaan Schmitz and Alexey Y. Kovalgin (University of Twente)

Deposition of thin layers containing Ga, C and N by sequential pulses of Trimethylgallium and Ammonia

Gallium nitride (GaN) is a semiconductor with broad applications in the (opto-)electronic industry. State-of-art integration of GaN in chips demands a nanometer-level control over its thickness, which can be achieved with atomic layer deposition (ALD) technique. Further, introducing carbon into GaN layers beyond the doping levels, to prepare a gallium carbon nitride (GaCN) material can be very interesting since carbon can be used to tune the electronic and optical properties of GaCN. Whereas carbon nitrides of boron, silicon and tungsten had been reported before, that of gallium has been hardly ever reported. In this work, we report on thin layers of GaCN on Si wafers deposited from trimethylgallium (TMG) and ammonia (NH3) precursors at temperatures between 400 and 600 ^{o}C. The precursors were sequentially introduced in a pulsed mode, i.e., without mixing them. Layers between 5 and 15 nm were deposited. The layer growth was monitored in-situ with spectroscopic ellipsometry (SE). Ex-situ characterization was performed with X-ray photoelectron spectroscopy (XPS), Grazing incidence X-ray diffraction (GIXRD) and scanning electron microscopy (SEM). An in-situ deposited aluminium nitride (AlN) buffer layer was found to be essential for depositing the GaCN layers, and deposition on bare Si wafers resulted in only 2 3 nm carbon-rich films, containing traces of gallium but no incorporation of nitrogen. The ratio between the Ga-, C- and N-contents, correspondingly to the layer growth rate, was found to be strongly dependent on the buffer layer thickness, the deposition temperature and the precursor pulse durations. The refractive index was found to increase, while the band-gap was found to decrease, for layers rich in carbon. These initial results on GaCN may in future lead to interesting applications in optoelectronic devices.

S18: Xingyu Liu, Lis. K. Nanver (University of Twente)

PureB: CVD Nanometer-Thin Pure Boron Layers for MEMS and VUV/EUV Photodiode Applications

The properties of nanometer-thin pure boron layers (PureB) deposited by chemical vapor deposition are being studied electrically and as barriers against chemical treatments. Here the focus is on the use as a barrier against tetramethyl ammonium hydroxide (TMAH) and potassium hydroxide (KOH)for the etching of Si. Deposition temperatures of 400 ^{o}C and 700 ^{o}C were applied to form layers of a few nanometer thick. Down to 2-nm thickness, they were all found to be resistant to these wet Si etchants. Patterning of the layers was achieved with resist masking and standard aluminum wet-etchant. The selectivity to Si was extremely high, much greater than 104. Cavities 70 μm deep were etched without measureable etching of the boron layers, and with $<$100$>$/$<$111$>$ etch-rate ratios of about 35 for TMAH and larger than 50 for KOH. Stress levels were measured to be 490 MPa tensile for 400 ^{o}C and 1250 MPa compressive for 700 ^{o}C deposition. Hundreds of micron wide membranes that remained intact were fabricated. Electrically, the PureB layer, fabricated by depositing pure boron on n-Si, forms the anode region of devices that function as p+n junction diodes, which can have very low dark-currents even though the photosensitive depletion

region is brought right up to the silicon surface. The robust B-to-Si interface properties have led to a fast qualification of PureB photodiodes for use in DUV/EUV lithography and metrology equipment. Electrical test structures were designed to create an easy-to-process, fast-turn-around time method to characterize the electrical quality of the interface with respect to PureB deposition parameters. Disruptions due to Si surface contamination, incomplete coverage with PureB, or some extra post-deposition steps caused an undesirable increase in the conductivity along the interface and dark current. Particularly at low deposition temperatures around 400 ^{o}C, the optimization of the processing parameters to avoid such increases becomes critical.

S19: A.J. Onnink, R.O. Apaydin, A.Y. Kovalgin (University of Twente)

Strategies to mitigate the ammonium halide contamination of an ALD/CVD reactor

Solid byproducts such as ammonium or pyridinium halides present a challenge in many atomic layer deposition (ALD) and chemical vapor deposition (CVD) processes based on Lewis acid/base chemistry. We report on the formation, migration and cleaning of ammonium bromide (NH4Br) as a byproduct of pulsed boron nitride (BN) deposition in a cold walled reactor. Combined in-situ spectroscopic ellipsometry (SE) and gas-phase infrared spectroscopy (FTIR) during a deposition cycle reveals the reaction HBr + NH3 $\rightarrow$ NH4Br. The NH4Br spreads throughout the reactor in the hours after deposition, as monitored by in-situ SE. Scanning electron microscopy (SEM) reveals that the NH4Br deposits as nanocrystals. We find 5 mechanisms that can be used drive the equilibrium towards net removal of NH4Br: heating, wet scrubbing, exposure to UV/Vis/NIR photons, exposure to an electron beam, and exposure to a H2/Ar plasma. Detailed in-situ monitoring of cleaning based on mass spectrometry (MS), FTIR and SE will be presented. We will give practical recommendations to minimize and clean the contamination.

S20: Juan J. Montero Rodríguez, W. Krautschneider (Instituto Tecnológico de Costa Rica, Hamburg University of Technology

Simulation and characterization of cells by impedance spectroscopy

Standard cell counting methods are time consuming and put stress on the cells by staining them with markers, reducing cell viability. Therefore, there is much interest in alternative fast and non-destructive methods. Impedance spectroscopy is an electrical approach that gives information about its permittivity and conductivity of a sample. Parameters such as the cell membrane capacitance or the conductivity of the cytoplasm affect the overall impedance, and are identified and extracted by mathematical modeling of the impedance data, using equivalent circuits based on electrochemical components such as resistors, capacitors, Warburg or constant-phase elements. The technique is used in the laboratory for identifying tumor cells in mice, comparing them with tissues from the liver, lung, brain, heart and leg. Other applications included in this work are the identification of bacteria in eye infections, the monitoring of the ripening process of fruits, and the detection of blood lactate concentration in athletes by using a skin sensor. These applications often require a portable measurement system. Therefore, a portable impedance spectroscopy system was designed and tested. A significant reduction of size, weight and power consumption of portable systems can be achieved by using an Application-Specific Integrated Circuit (ASIC). Three ASICs were used to assemble miniaturized devices. The ASIC 1 operates at frequencies below 40 kHz, and it is used for cell growth experiments. The ASIC 2 and ASIC 3 operate at frequencies close to 40 GHz and are suitable for impedance recording above the water relaxation frequency. It is concluded that the method works and can be effectively integrated into an ASIC for field experiments where portability is required. The method can be further improved by 4-terminal measurements. For extension of the method to millimeter-wave frequencies, full electromagnetic simulation of the chip has been carried out, and electrodes and interconnections have been adjusted accordingly.

[1] Juan J. Montero-Rodriguez, Adolfo J. Fernández-Castro, Dietmar Schroeder, Wolfgang Krautschneider. Development of an impedance spectroscopy device for on-line cell growth monitoring. Electronics Letters, 2017.

Ravelijn 1501

Location

The SAFE 2018 workshop will take place in two locations, at walking distance (approximately 500 m, 7 min) from each other:

Lectures, presentations, etc. will be in:
Building Ravelijn (RA, number 10 on the campus map)
Room RA1501

Posters, lunch & dinner will be in:
Hotel Drienerburght (DR, number 44 on the campus map)

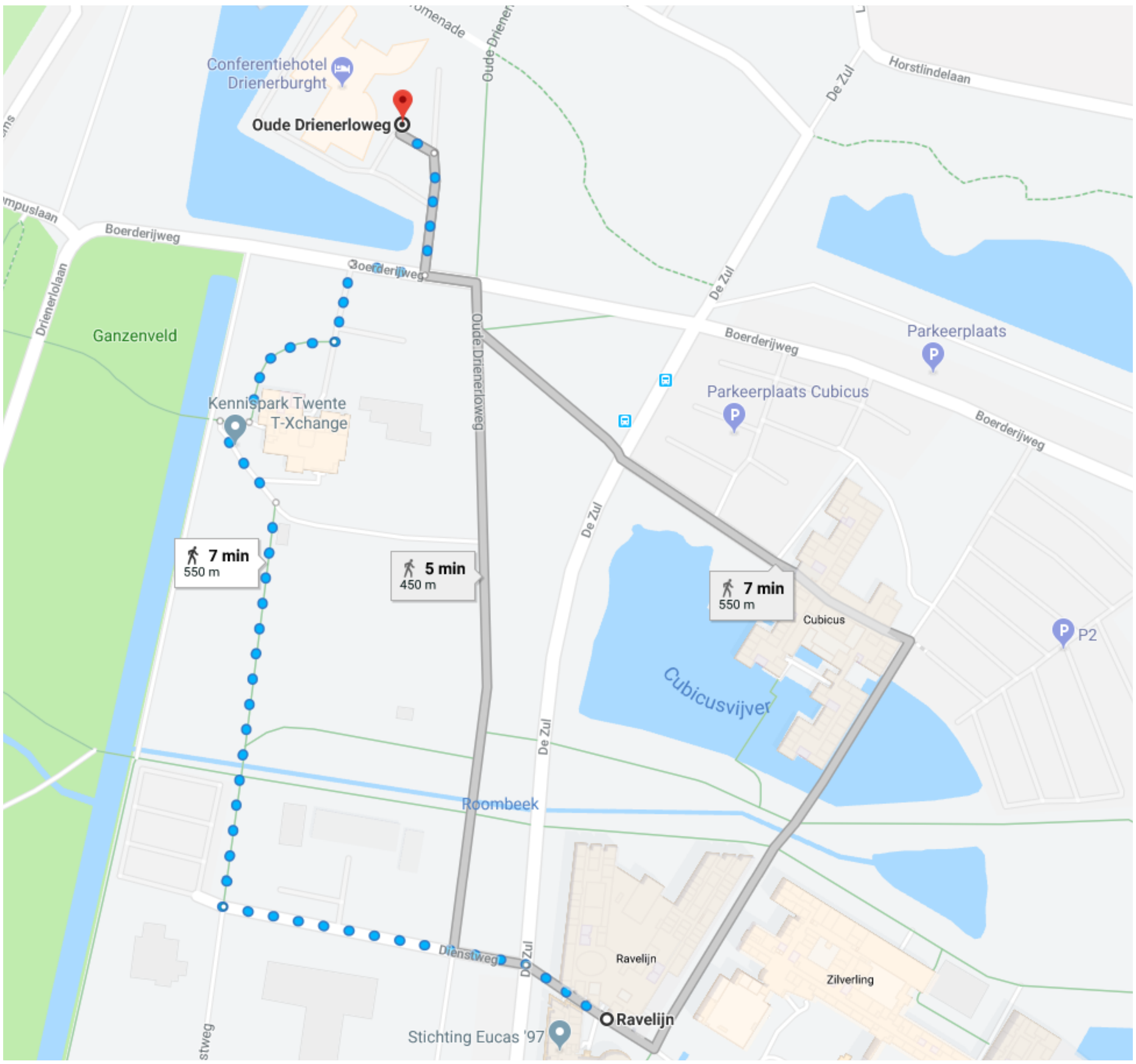

MAP OF THE UNIVERSITY OF TWENTE

0 O&O plein (OO)
2 Spiegel (SP)
3 Vleugel (VL)
4 Carillon (CN)
5 Garage (GA)
6 Paviljoen (PA)
7 Seinhuis (SH)
8 Hogedruklab (HD)
9 Citadel (CI)
10 Ravelijn (RA)
11 Zilverling (ZI)
12 Waaier (WA)
13 Hal B (HB)
14 Teehuis (TH)
15 Carré (CR)
16 Nanolab (NL)
17 The Gallery (GY)
18 Technohal (TL)
20 Horsttoren (HT)
21 Horstring (HR)
22 Westhorst (WH)
23 Kleinhorst (KH)
24 Noordhorst (NH)
26 Oosthorst (OH)
27 Meander (ME)
28 Zuidhorst (ZH)
29 Buitenhorst (BH)
30 Keet (KT)
31 Windpark (WP)
32 BMC (BI)
39 Chalet (CT)
40 Erve Holzik (ER)
41 Cubicus (CU)
42 Faculty Club (FC)
43 Schuur (SR)
44 Drienerburght (DR)
45 Hogekamp (HO)
46 High Tech Factory (HTF)
47 Vrijhof (VR)
48 Bastille (BA)
49 Sportcentrum (SC)
51 Shopping centre/Sky (SK)
53 Box (BO)
56 Openluchttheater (OUT)
57 Zwembad (ZW)
58 Sleutel (SL)
59 Mondriaan (MO)
60 Vlinder (VI)
61 Linde (LI)
62 Boerderij Bosch (BB)
63 Stall (ST)
63 Blokhutten (BL)
64 Tennispark (TP)
65 Logica (LO)
66 BTC (BTC)

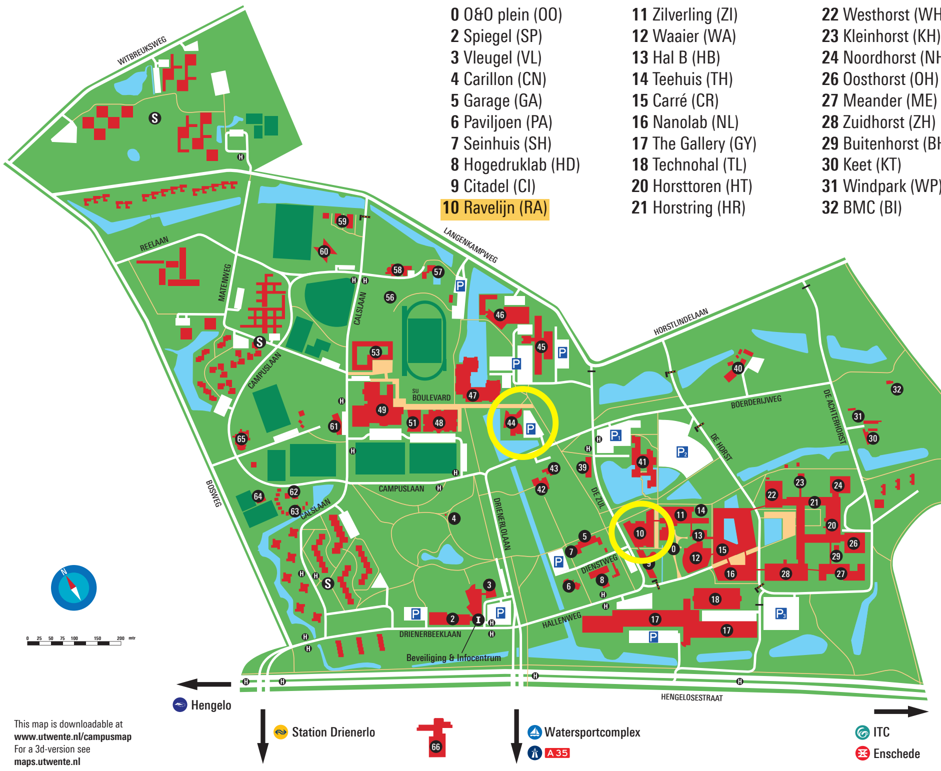

- Security service office
- Student housing
- Bus stop
- Parking
- Barrier
- Closed road

This map is downloadable at
www.utwente.nl/campusmap
For a 3d-version see
maps.utwente.nl

UNIVERSITY OF TWENTE.

Destination	Building number
FACULTIES	
Faculty of Behavioral Sciences (GW)	9, 39, 41
Educational Science and Technology; Psychology, Communication Studies; Philosophy of Science, Technology and Society; Teacher's training	
Faculty of Electrical Engineering, Mathematics and Computer Science (EWI)	9, 11, 15
Electrical Engineering; Applied Mathematics; Business Information Technology; Creative Technology; Telematics; Computer Science; Embedded Systems; Mechatronics; Human Media Interaction; Systems and Control	
Faculty of Engineering Technology (CTW)	20, 21, 22, 45
Civil Engineering; Industrial Design Engineering; Sustainable Energy Technology; Mechanical Engineering; Construction Management & Engineering	
Faculty of Science and Technology (TNW)	15, 20, 21, 24, 26, 27, 28
Advanced Technology; Biomedical Technology; Chemical Engineering; Nanotechnology; Applied Physics; Technical Medicine	
School of Management and Governance (MB)	10
Business Administration; Public Administration; European Studies; Health Sciences; Industrial Engineering and Management	

Destination	Building number
INSTITUTES	
CTIT Centre for Telematics and Information Technology	11
ELAN Institute	41
MIRA Institute for Biomedical Technology and Technical Medicine	28
IGS Institute for Governance Studies	10
MESA+ Institute for Nanotechnology	15, 16
SERVICE DEPARTMENTS AND FACILITIES	
Acasa (student housing)	58
Bicycle Workshop (De 2e Versnelling)	53
Campus Company (reservations & events)	47
Children's day care centre 'Vlinder' (Catalpa)	60
Conference Hotel (Drienerburght)	44
Culture Centre, Vrijhof	47
Delivery	5
Dentist (Huizinga)	58
Executive Board (CvB)	3
Facility Department (FB)	6
Faculty Club	42
Financial and Economic Affairs (FEZ)	2
General Affairs (AZ)	2
General Practitioner	58
Hair Dresser (De Barreboks)	51
High Tech Factory	46
Hotel Drienerburght	44
Hotel Logica	65
Human Resources (HR)	2
ICT Service Centre (ICTS)	(2, 17) 20
International Office	48
Kennispark Twente (via parking Hengelosestraat)	72

Destination	Building number
Library & Archive (B&A)	47
Mail Room	5
Main Entrance	2, 3
Marketing & Communication Department (M&C)	2
O&O square	0
Physiotherapy (Polman)	49
Professional Learning & Development (PLD)	10
Restaurants	12, 42, 47
Science Shop (WeWi)	17
Security & Infocentre	2
Shops (COOP Supermarket)	51
Sports Centre	49
Strategy & Policy (S&B)	2
Student Counselling Service	47
Student Counsellors	47
Student & Education Service Centre (S&O)	47
Student Psychologists	47
Student Restaurant (Mensa)	12
Student Services	47
Student Union	48
Studium Generale (SG)	47
Study Information Office (SI)	2
Swimming Pool	49, 57
Theatercafé Vrijhof	47
Twente Academy (Young)	48
Twente Graduate School (TGS)	10
Unionshop	48
UT-Nieuws	47
Vestingbar	48
Xerox Service Center	13

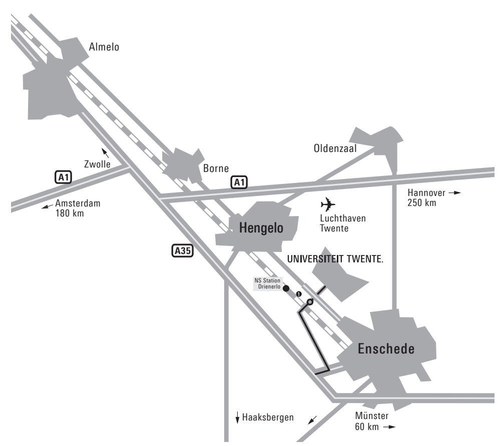

How do you get to the University of Twente?

BY CAR
From the A1 motorway, take the A35 motorway in the direction of Enschede
Take the exit 'Enschede – West / Universiteit' (exit no. 26)
Follow the signs for 'Universiteit'

1 Route description to the ITC faculty
After the roundabout, turn right (follow 'centrum')
At your right-hand side you will see the ITC after 3 km (Hengelosestraat 99)

BY TRAIN / BUS

From Enschede railway station:	line number 1 in the direction of 'Universiteit Twente' line number 8 in the direction of Hengelo-Noord line number 9 in the direction of Hengelo
From Enschede Drienerlo railway station:	line number 1 in the direction of 'Universiteit Twente'
From Hengelo railway station:	line number 9 in the direction of Enschede line number 15 in the direction of 'Universiteit Twente' line number 16 in the direction of 'Universiteit Twente'

For more information, please call the information service number for Public Transport: 0900-9292

Hotels

ACCOMMODATIONS IN ENSCHEDE

Some hotels are listed below for your convenience.

Drienerburght Conferentiehotel - on campus

Drienerburght is convenient located as it is in the centre of the UT-campus and also is the place where part of the SAFE2018 workshop is hosted. They do have a limited number of discounted rooms. To book a room at Conference hotel Drienerburght go to their website, email them or call them (053 4802666). Please mention you will attend SAFE.

Intercity Hotel - citycenter

Please inquire for prices by sending an email to Marlies Rijnberg mentioning SAFE2018. Alternatively you may book through their website for regular offerings.

Hotel De Broeierd Enschede - across the campus

Double room (splitlevel) € 89,50 per night per person excluding breakfast ad € 12,50

DeLuxe room € 99,50 per night excluding breakfast ad € 12,50

To book a room at Hotel De Broeierd, you can send an e-mail to info@fletcherhotelenschede.nl citing SAFE.

* prices are excluding € 1,27 city tax per person, per night